ARTICLE

Integrated Super Computational Prediction of Liquid Droplet Impingement Erosion

Jun ISHIMOTO [1,*], Shinji AKIBA [2],
Kazuhiro TANJI [2] and Kazuo MATSUURA [3]

[1] *Institute of Fluid Science, Tohoku University, 2-1-1, Katahira, Aoba-ku, Sendai, Miyagi 980-8577, Japan*
[2] *Tohoku Electric Power Co., Inc., 1-7-1 Honcho, Aoba-ku, Sendai, Miyagi 980-8550, Japan*
[3] *International Advanced Research and Education Organization, Tohoku University, Sendai 980-8578, Japan*

The 3-D structure of the high-speed liquid droplet-vapor two-phase pipe flow characteristics and LDI erosion behavior in a power plant is numerically predicted by integrated parallel CFD analysis. Governing equations of two-phase flow taking into account the condensed liquid-droplet generation, vapor-liquid phase change in conjunction with the coupled Euler-Lagrange dispersed two-fluid model were developed. Furthermore, data on such factors as the droplet impingement pressure, droplet diameter, and pipe thinning rate (erosion rate) by LDI which are difficult to confirm by experiment, were acquired.

KEYWORDS: liquid droplet impingement (LDI), droplet condensation, erosion, pipe thinning, multiphase flow, CFD, integrated parallel super-computation, Euler-Lagrange coupled model

I. Introduction

Liquid droplet impingement (LDI) erosion is closely related to the pipe wall thinning by aged deterioration in actual work of the nuclear power plant.[1]

In the present study, 3-D structure of the high-speed liquid droplet-vapor two-phase pipe flow characteristics and LDI erosion behavior in a power plant is numerically predicted by integrated parallel CFD analysis. The most important point in this study is that the liquid-droplet generation by condensation from steam vapor-phase is precisely taken into account, and the growth of the droplet diameter accompanying with the surrounding high speed vapor flow is successfully computed by phase change model.

Governing equations of two-phase flow taking into account the vapor-liquid phase change in conjunction with the coupled Euler-Lagrange dispersed two-fluid model were developed. Furthermore, data on such factors as the droplet impingement pressure, droplet diameter, and pipe thinning rate by LDI which are difficult to confirm by experiment, were acquired.

According to the present analysis, the numerically obtained data of the droplet impingement pressure, and pipe wall thinning rate by LDI were found to be controlled by the generation and motion of micro liquid-droplets. The micro liquid-droplets are generated coincident with the vapor-phase condensation due to the transport of latent heat of vaporization. These vapor-liquid droplet phase change is mainly caused by the rapid expansion of high-speed vapor-phase flow through the orifice.

The complex pipeline geometry and high-speed thermal two-phase flow characteristics of the nuclear power plant was virtually reproduced on the super computer by using this computational system, and it would be possible to predict the pipeline trouble related with LDI in advance. This computational system can substantially decrease the time cost and human cost which is required for reactor maintenance inspection, and also the system can realize quite safety pipeline risk management in the nuclear power generation.

II. Governing Equations

Governing equations of two-phase flow taking into account the vapor-liquid phase change in conjunction with the coupled Euler-Lagrange dispersed two-fluid model were derived as follow.

1. Equations of Continuum Phase (Vapor Phase)

Mass conservation equation:

$$\frac{\partial \rho}{\partial t} + \nabla \cdot (\rho U) = S_m \tag{1}$$

Momentum equation:

$$\frac{\partial (\rho U)}{\partial t} + \nabla \cdot (\rho U U) - \nabla \cdot \left[\mu \left(\nabla U + (\nabla U)^T \right) \right]$$
$$= -\nabla \left(P + \frac{2}{3} \mu \nabla \cdot U \right) + S_U \tag{2}$$

Energy equation:

$$\frac{\partial \rho h}{\partial t} + \nabla \cdot (\rho h U) - \nabla \cdot (\alpha \nabla h) = \frac{Dp}{Dt} + S_h \tag{3}$$

Equation of state:

$$\rho = \rho (P, T) \tag{4}$$

*Corresponding author, E-mail: ishimotojun@ieee.org

where the source terms in Eqs. (1)–(3) include the effect of mass, momentum and energy transfer between droplet-phase and surrounding vapor phase. The constitutive equations of source term are derived as following equation:

$$S_m = -\left\{\sum_m^{mp}\sum_n^{nt}\left[\left(\dot{m}_p\right)_{mn}^{t+\Delta t} - \left(\dot{m}_p\right)_{mn}^{t}\right]\right\}/V_{CV}$$

$$S_U = -\left\{\sum_m^{mp}\sum_n^{nt}\left[\left(\dot{m}_p U_p\right)_{mn}^{t+\Delta t} - \left(\dot{m}_p U_p\right)_{mn}^{t}\right]\right\}/V_{CV} \quad (5)$$

$$S_h = -\left\{\sum_m^{mp}\sum_n^{nt}\left[\left(\dot{m}_p h_p\right)_{mn}^{t+\Delta t} - \left(\dot{m}_p h_p\right)_{mn}^{t}\right]\right\}/V_{CV}$$

where $\dot{m}_p$ is the droplet-phase mass generation density, U_p is the droplet-phase velocity.

$$h_p = h_b + \frac{3\left(\sigma_p - T_p \dfrac{d\sigma}{dT}\right)}{\rho_p r} + \frac{u_p^2}{2} \quad (6)$$

where the terms of r.h.s is the enthalpy, surface enthalpy and momentum energy.

2. Turbulence Model

The $k-\omega$ model is employed to formulate the two-phase turbulence equations.[2]

$$\frac{\partial \rho k}{\partial t} + \nabla\cdot(\rho U k) - \nabla\cdot\left((\mu+\sigma_k\mu_t)\nabla k\right) = P_k - \beta^*\rho k\omega \quad (7)$$

$$\frac{\partial \rho\omega}{\partial t} + \nabla\cdot(\rho U\omega) - \nabla\cdot\left[(\mu+\sigma_\omega\mu_t)\nabla k\right]$$
$$= \alpha\rho S^2 - \beta\rho\omega^2 + 2(1-F_1)\rho\sigma_{w2}\frac{1}{\omega}\nabla k\cdot\nabla\omega \quad (8)$$

3. Equations for Dispersed Phase (Droplet Phase)

Momentum equation:

$$\frac{d(m_d u_d)}{dt} = -\frac{\pi D^2}{8}\rho C_D |u_d - u|(u_d - u) + m_d g \quad (9)$$

$$C_D = \begin{cases} \dfrac{24}{Re_d}\left(1+\dfrac{1}{6}Re_d^{2/3}\right) & Re < 1000 \\ 0.424 & Re > 1000 \end{cases} \quad (10)$$

$$Re_d = \frac{\rho|u_d - u|D}{\mu} \quad (11)$$

To evaluate the initially nucleated condensed droplet radius, the classical nucleation theory for water droplets from subcooled vapor to the bulk liquid is employed.

$$r_* = \frac{2\sigma}{\rho_l RT_v \ln S} = \frac{2\sigma T_s(p)}{\rho_l h_{vl}\Delta T} \quad (12)$$

$$J = \frac{q_c}{1+\eta}\left(\frac{2\sigma}{\pi m^3}\right)^{0.5}\frac{\rho_v}{\rho_l}\exp\left(-\frac{\Delta G^*}{K_b T_v}\right) \quad (13)$$

$$\Delta G^* = \frac{16\pi\sigma^3}{3\rho_l(\Delta G_b)^2} = \frac{4}{3}r_*^2\pi\sigma \quad (14)$$

$$\eta = 2\frac{\gamma-1}{\gamma+1}\frac{h_{vl}}{RT_v}\left(\frac{h_{vl}}{RT_v} - 0.5\right) \quad (15)$$

where r^* is the Kelvin-Helmholtz critical nucleate radius, K_b is Boltzmann's constant, J is the nuclei generation rate of liquid droplets, q_c is the condensation coefficient, and $q_c = 1$ is applied. η is the nonisothermal correction factor,[3] m is the mass of a single molecule of mercury, γ is the surface tension, R is the gas constant, T_s is the saturation temperature.

By introducing the formulation of the growth process for condensed droplets, we assume that the growth rate of a droplet is controlled by the rate at which the enthalpy of condensation can be conducted away from the droplets to the bulk liquid.[4]

Under that assumption, the equation of the growth process for a condensed droplet is derived as following equations.[5,6]

$$\frac{\partial r}{\partial t} = \frac{k_v\Delta T(1-r_*/r)}{\rho_l h_{vl}\left(r+1.89(1-v)\lambda_v/Pr_v\right)} \quad (16)$$

$$\lambda_v = \frac{1.5\mu_v\sqrt{RT_v}}{p} \quad (17)$$

$$v = \frac{RT_s(p)}{h_{vl}}\left[\beta - 0.5 - \frac{2-q_c}{q_c}\frac{\gamma+1}{2(\gamma-1)}\frac{RT_s(p)}{h_{vl}}\right] \quad (18)$$

Discrete Droplet Model; DDM and TAB model[7] used in KIVA-II are applied to consider the breakup and deformation of droplet.[8] The unsteady change of droplet radius is calculated by Eq. (16) in consideration with the vaporization and condensation rate caused by energy exchange of different phase.

4. Evaluation of LDI Erosion Rate

The erosion rate is evaluated as following equation.[9]
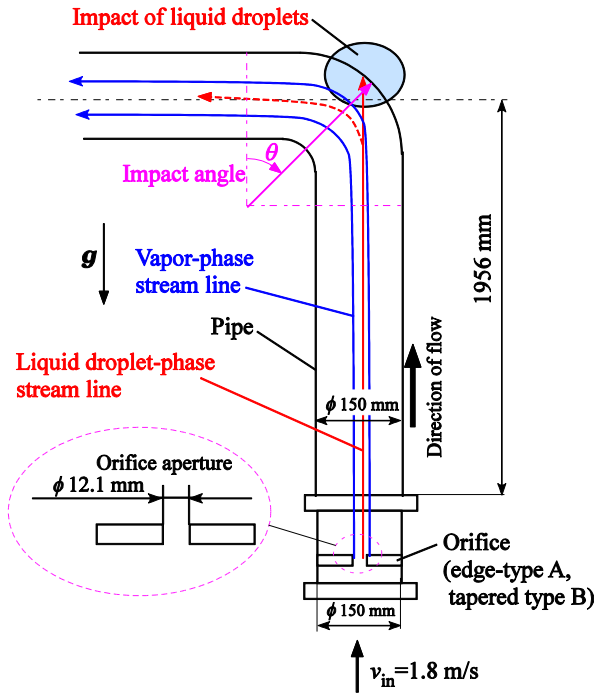
$$E = K_m m_p f(\theta)V_p^n \quad (19)$$

where E is the erosion rate (kg/s), m_p the particle flux (kg/s), Km the material constant (m/s), θ the droplet impact angle, $f(\theta)$ the function of impact angle, V_p the particle impact velocity and superscript n the velocity exponent, normally between 2.5 and 3.0.
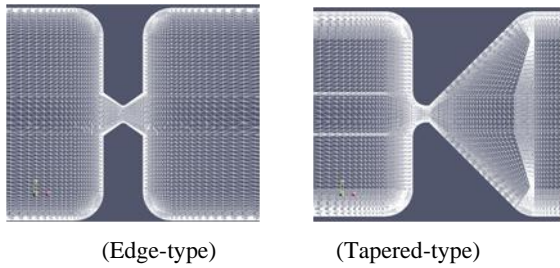
III. Numerical Procedures

1. Computational Domain and Numerical Conditions

Figure 1 depicts the major computational system expected in the present calculation. The computation has been performed in the two-types of orifice mesh ("edge-type A" and "tapered type B"). The computational geometry is referenced as same shape as actual pipe system of nuclear power plant in Japan.

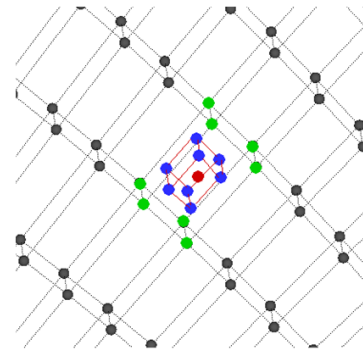For initial numerical conditions, a constant velocity and

Impact of liquid droplets

Impact angle θ

g

Vapor-phase stream line

Pipe

1956 mm

Direction of flow

ϕ 150 mm

Liquid droplet-phase stream line

Orifice aperture ϕ 12.1 mm

Orifice (edge-type A, tapered type B)

ϕ 150 mm

v_{in}=1.8 m/s

(a) Elbow model for analysis

(Edge-type)   (Tapered-type)

(b) Used two types of orifice shape

Fig. 1   Computational system employed

Fig. 2   Droplet insertion model for control volume

tion in two-phase steam flow.[5,6]

2. Droplet Insertion Method to Calculation Cell

As shown in **Fig. 2**, the computational cell unit which is surrounded in the green point is control volume. When as for degree of subcooling of this cell volume approaching to critical value, (liquid drop formation rate of $J \geq 10^{15}$), one parcel group (red point which locates at grid central) is inserted in the center of control volume. $J \geq 10^{15}$ is the threshold of nucleation rate evaluated by obtained subcooling rate just downstream of orifice throat section in reference to Bakhtar's analysis.[11]

In order to compute precisely, we applied the method of inserting some parcel groups in the control volume. For example, it inserts eight particle groups (indicating with the blue point) in eight octant centers in the control volume.
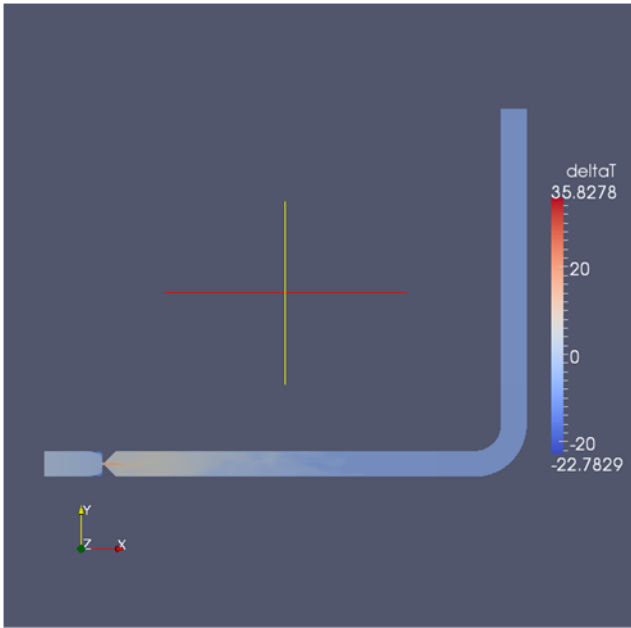
The number of droplet particle which is included in one parcel group is defined as follows:

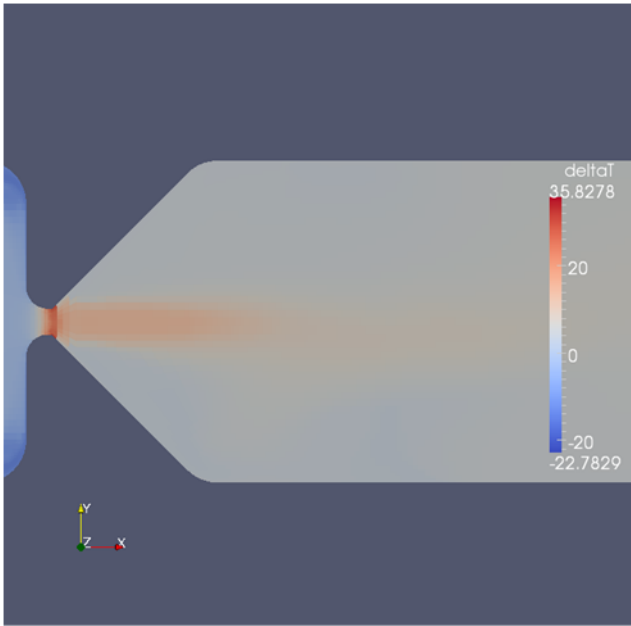$$\dot{n}_p = \frac{N_P}{n_p} = \frac{JV_{CV}}{n_p} \tag{20}$$

where $\dot{n}_p$ is the number of droplet in the parcel group, N_p is the total number of droplet inserting to the control volume, n_p is the number of parcel group, J is the droplet generation rate, V_{CV} is the volume of control volume.

IV. Results and Discussion

To investigate the micron size liquid droplet formation precisely, the vapor subcooling is numerically calculated. **Figure 3** shows the magnitude of subcooling in the condition of the outlet pressure $p = 100$ kPa of tapered type orifice. As shown in Fig. 3, the steam flow into from the entrance, to be compressed and accelerated at the orifice, then it expands in the exit portion of orifice. With this process, pressure and temperature of the steam is rapidly decreasing. Because the water which is used at the nuclear power plant is quite high purity, there are few condensation nucleus in that state of the steam, micro-droplet condensation cannot immediately occur even with when it exceeds the saturation condition. Thus, the steam has a possibility of becoming subcooling state, namely the state is subcooling of $\Delta T > 0$. When degree of subcooling becomes large, also liquid drop formation rate J of the subcooled steam becomes

temperature profiles are applied to the inlet section and a constant pressure condition is applied to the outlet section. The nonslip condition for prescribed velocity is applied to the wall of inflow section and orifice throat section. A free-slip condition for the prescribed velocity is applied to the surrounding wall outlet domain of the nozzle throat.

To find the available numerical condition to activate the condensed droplet formation, the four outlet pressure conditions of 24.7 kPa, 54.7 kPa, 89.7 kPa and 100 kPa are applied to perform the parallel super computation. In the initial numerical condition, the saturated vapor condition is applied to whole internal region of pipe, inlet velocity $U_{in} = 1.8$ m/s is applied to the inlet of pipe. To evaluate the erosion rate in the present nuclear plant, the pressure $p_{out} = 100$ kPa is applied to the outlet of pipe.

To compute the present system, we developed an original CFD solver, named ``*phaseChangeParcelFoam,*'' using the OpenFOAM finite volume CFD open source code[10] based on the extended form of *dieselFoam* and *twoPhaseEulerFoam*. The CFD code validation has been conducted by comparison regarding with the previous study of condensa-

(Overall profile of tapered type orifice to bent section)

Fig. 4   Particle diameter profiles in the elbow pipe

(Close-up view of throat section of tapered type orifice)

Fig. 3   Magnitude of subcooling in the condition of the outlet
pressure $p = 100$ kPa of tapered type orifice

(a) Numerical result

large. By using critical liquid droplet nucleation rate, the possibility of the liquid droplet generation in the subcooled steam is considered.

When the steam condenses, many condensation nucleus are formed, then they become to micro-liquid droplets. Simultaneously, because the degree of subcooling is $\Delta T > 0$, the formed the micro-liquid droplets are enhanced to grow up. Just downstream of orifice exit portion, ΔT approaches to maximum 35.83 K, it is especially found that the high degree of subcooling region is formed around the pipe central axis of the orifice. By trying computation under several numerical conditions, it is ascertained that the condensation
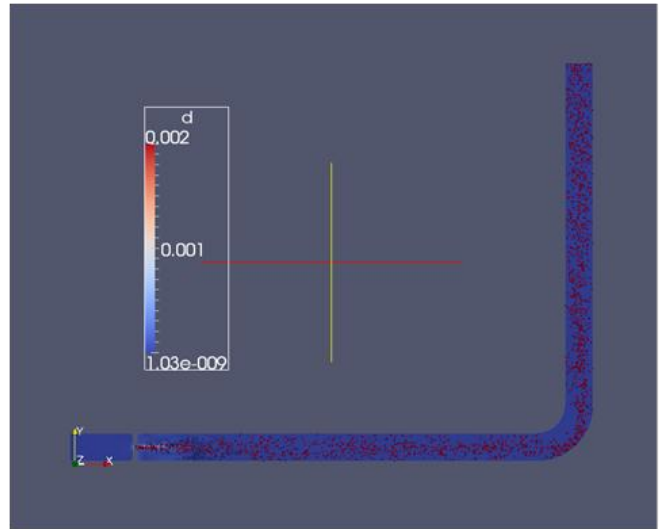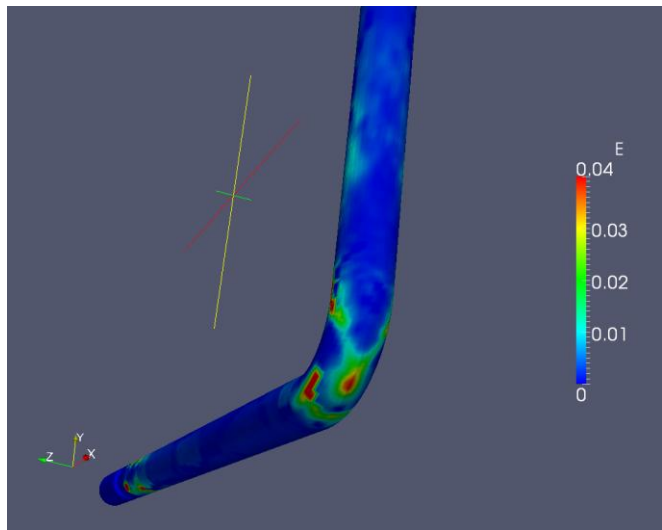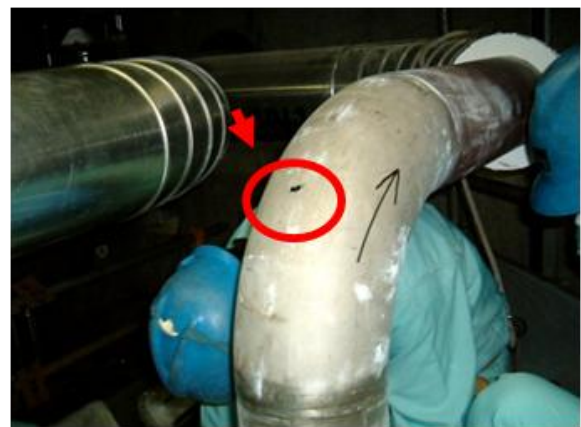

(b) Actual image of LDI erosion phenomena

Fig. 5   Numerical result of LDI erosion rate and actual image of LDI erosion phenomena.

Table 1 Effect of orifice shape type on droplet particle impact angle and the droplet maximum impact velocity

	Impact angle θ	Maximum impact velocity $u_{d\max}$
Edge-type	72.83 deg.	511.16 m/s
Tapered-type	78.68 deg.	445.38 m/s

of vapor occurs in the condition of the outlet pressure above the 100 kPa. Thus the following numerical results are conducted in the condition of 100 kPa outlet pressure.

Figure 4 shows the particle diameter profiles in the elbow pipe. It is clarified that the diameter size of 1.0 to 2.0 mm liquid droplet particles mainly impact to the bent portion of the pipe. Because of the high speed droplet motion ($U_{\max} = 482$ m/s), Weber number exhibits large value of $We = 3.2 \times 10^6$. The initial nucleation radius of droplet has the small value, however, the droplet radius grows up passing through the orifice throat caused by the rapid condensation with adiabatic expansion of vapor phase.

It can be estimated that those size order of droplet particles becomes the principal factor which causes the LDI erosion.

Table 1 shows the droplet particle impact angle θ and the droplet maximum impact velocity $u_{d\max}$ of normal component at the elbow bent portion in edge-type and tapered-type orifice, respectively. In the condition of tapered-type orifice, it is found that the droplets impact at upstream than edge-type, and the value of $u_{d\max}$ is smaller than edge-type's case. As a result, it can estimate that the LDI erosion is controlled to decrease in the case of tapered-type orifice above 100 kPa of outlet pressure condition.

Figure 5 shows the numerical result of LDI erosion rate E and actual image of LDI erosion phenomena. The magnitude of erosion rate extensively increases around the elbow central of bent portion. The large size particle (about 2.0 mm) causes the LDI erosion by high-speed impact pressure of its inertia force. The erosion is also caused by the rebounded liquid-droplets flow around the bent section.

Furthermore, erosion rate increases just downstream region of the orifice throat. It is considered that the erosion is caused by the liquid-droplets impinging which follow to the counterflow of the steam flow downstream the orifice.

The photograph in Fig. 5(b) shows actual LDI erosion which it occurs in the elbow bent portion which is used at the nuclear power plant. By comparing the actual phenomenon with numerical result, it is found that the aspect of LDI erosion reasonably agree with both the numerical results and the actual fact.

Therefore, the developed numerical code can be possible to predict the location of erosion occurrence and erosion rate qualitatively. These results confirm the validity of the CFD analysis employed in this study and that CFD can be applied to design safety optimization of a total piping system of nuclear power plants.

V. Conclusion

1. To investigate the micron size liquid droplet formation precisely, the vapor subcooling is numerically calculated. It is ascertained that the condensation of vapor occurs in the condition of the outlet pressure above the 100 kPa condition.
2. It is clarified that the diameter size of 1.0 to 2.0 mm liquid droplet particles mainly impact to the bent portion of the pipe. It can be estimated that those size order of droplet particles becomes the principal factor which causes the LDI erosion.
3. It can estimate that the LDI erosion is controlled to decrease in the case of tapered-type orifice above 100 kPa of outlet pressure condition.
4. By comparing the actual phenomenon in nuclear power plant with numerical result, it is found that the aspect of LDI erosion reasonably agree with both the numerical results and the experimental results. Therefore, the developed numerical code can be possible to predict the location of erosion occurrence and erosion rate qualitatively.

References

1) R. Morita, F. Inada, K. Yoneda, "Development of Evaluation System for Liquid Droplet Impingement Erosion (LDI)," *ASME Conf. Proc. 2009*, 881 (2009), DOI: 10.1115/PVP2009-77557.
2) F. R. Menter, M. Kuntz, R. Langtry, ``Ten Years of Industrial Experience with the SST Turbulence Model,'' *Turbulence, Heat and Mass Transf. 4*, Begell House, Inc. (2003).
3) A. G. Gerber, A. Mousavi, ``Application of quadrature method of moments to the polydispersed droplet spectrum in transonic steam flows with primary and secondary nucleation," *Appl. Math. Modeling*, **31**, 1518–1533 (2007).
4) C. A. Moses, G. D. Stein, ``On the growth of steam droplets formed in laval nozzle using both static pressure and light scattering measurements,'' *Trans. ASME J. Fluids Eng.*, **100**, 311–322 (1978).
5) J. B. Young, ``Two-dimensional, nonequilibrium wet-steam calculations for nozzles and turbine cascades." *Trans. ASME J. Turbomach.*, **114**, 569–578 (1992).
6) J. B. Young, ``The spontaneous condensation of steam in supersonic nozzles." PCH *PhysicoChem. Hydrodyn.*, **3**, 57–82 (1982).
7) A. D. Gosman, R. J. R. Johns, ``Computer Analysis of Fuel-Air Mixing in Direct-Injection Engines, " *SAE Technical Paper*, 800091 (1980).
8) A. A. Amsden, T. D. Butler, P. J. O'Rourke, ``The KIVA-II Computer Program for Transient Multidimensional Chemically Reactive Flows with Sprays," *SAE Technical Paper*, 872072 (1987).
9) L. Nokleberg, T. Sontvedt, ``Erosion of Oil and Gas Industry Choke Valves Using Computational Fluid Dynamics and Experiment,'' *Int. J. Heat and Fluid Flow*, **19**, 636-643
10) OpenCFD, http://www.openfoam.com/
11) F. Bakhtar, J. B. Young, A. J. White, D. A. Simpson, `` Classical Nucleation Theory and Its Application to Condensing Steam Flow Calculations,'' *Proc. Inst. Mech. Eng., Part C: J. Mech. Eng. Sci.*, **219**, 1315-1333 (2005).